JURNAL REKAYASA PROSES
VOLUME 17, NUMBER 1, 2023, xx–xx

RESEARCH ARTICLE

Removal of metronidazole from simulated wastewater using Fe/C catalyst with a combination of heterogenous Fenton and ozonation

Budi Satria Panandita[1,2], Imam Prasetyo[1,2], Teguh Ariyanto[1,2,*]

[1]Department of Chemical Engineering, Universitas Gadjah Mada, Jl. Grafika 2,Yogyakarta, 55281, Indonesia
[2]Carbon Material Research Group, Department of Chemical Engineering, Faculty of Engineering, Universitas Gadjah Mada, 55281 Yogyakarta, Indonesia

Received 22 June 2022; revised 02 September 2022; accepted 01 May 2023

OBJECTIVES This study examined roles of iron oxide/porous carbon material (Fe/C) for removing metronidazole in simulated wastewater by adsorption and then followed by a degradation using advanced oxidation process (H_2O_2, O_3 and combination of H_2O_2/O_3). METHODS Fe/C was produced by an impregnation of iron oxide precursors during resorcinol-formaldehyde synthesis followed by pyrolysis at 800 °C. For comparison, blank carbon (without iron loading) was also synthesized. The properties of porous carbon were investigated by SEM-EDX, and N_2-sorption analyzer. Blank carbon and Fe/C featured the specific surface area of 755 m^2g^{-1} and 394 m^2g^{-1}, respectively. The loading of iron oxide altered the pore structures of material. RESULTS The adsorption isotherm data were followed by the Langmuir isotherm model with metronidazole uptake up to 46.07 mg g^{-1} and 39.97 mg g^{-1} at 30 °C by Fe/C and blank carbon. The degradation study was then carried out with catalyst dosage of 0.1 g/100 mL solution and 120 min reaction time at 30 °C. CONCLUSIONS It is noticeably that, the degradation of metronidazole was better when a combination of H_2O_2/O_3 was employed, compared with an individual of H_2O_2 or O_3. Regarding the stability, Fe/C maintained its high activity upon four consecutive runs.

KEYWORDS Advanced oxidation; iron oxide; metronidazole; porous carbon

1. INTRODUCTION

The development of pharmaceutical industries could create problems related to environmental affecting aquatic ecosystems and human health. Pharmaceutical contaminants have potentially raised concerns since they are toxic to aquatic organisms at trace concentrations (Mirzaei et al. 2017). Therefore, these compounds can not only be found in sewage treatment units, but its presence has been detected in groundwater (Patel et al. 2019), surface water, and seawater (Costanzo et al. 2005). Some of the doses used in medical procedures are not absorbed (Balarak et al. 2020). They are wasted by humans and accumulate in waste disposal units (Malakootian et al. 2019). The presence of these drugs can affect water quality. Several hazards include the development of antibiotic-resistant microbes in the aquatic environment (Gadipelly et al. 2014), changes in fish reproduction due to the presence of estrogenic compounds (Escher et al. 2010) and inhibition of photosynthesis in algae (Munoz et al. 2017).

Metronidazole is an antibiotic in the family of nitroimidazole. The molecular structure is shown in Figure 1. Metronidazole has a three-dimensional size of X = 0.668, Y = 0.627 and Z = 0.262 nm (Carrales-Alvarado et al. 2014). This compound is commonly used to treat infections caused by protozoa and anaerobic bacteria (Goolsby et al. 2018). These compounds have high solubility in water and difficult to degrade naturally (Johnson and Mehrvar 2008). In recent years, Adsorption is a widely used as treatment procedure for removal organic pollutants like antibiotic (Balarak et al. 2020). Adsorption is an effective method to remove metronidazole from aqueous solutions (Ighalo et al. 2020). However, the adsorption method only moves components from liquid to solid phase. For this reason, the degradation process is considered used as alternative processes to remove pharmaceuticals in the adsorbent. The degradation processes are currently being developed to remove pharmaceuticals compounds are advance oxidation processes (AOPs). This method have been widely used to remove organic pollutants such as antibiotics by produce hydroxyl radicals (Cuerda-Correa et al. 2020).

Many studies have been focused on the preparation of adsorbent and catalysts. It has to be mentioned that it is

*Correspondence: teguh.ariyanto@ugm.ac.id

© The Author(s) 2023, under the terms of a CC BY-SA 4.0 license.

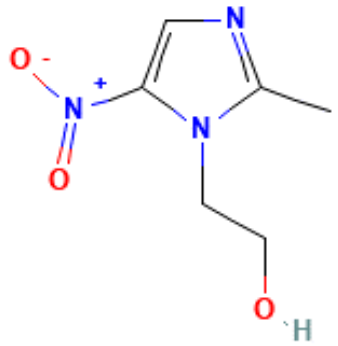

FIGURE 1. Molecular structure of metronidazole (Carrales-Alvarado et al. 2014).

difficult to separate the solid catalyst from aqueous suspension when using a homogenous system AOPs. Porous carbon is considered one of the most promising support materials because it has outstanding properties such as good physical and chemical stability (Ariyanto et al. 2019), high specific surface area (500-2000 m^2/g) (Mohd Zawawi et al. 2021), well-developed pore structure, and good surface chemistry (Prasetyo et al. 2013). Porous carbon could be used as a catalyst carrier medium in advanced oxidation processes (Amelia et al. 2020). Therefore, many works have been devoted to studying different carbon materials as catalytic support for removal metronidazole (Nasseh et al. 2020; Seidmohammadi et al. 2021). However, the pore structure of porous carbon as a heterogeneous catalyst for the degradation process of metronidazole has not been studied in depth before. The influence of the porous carbon structure as a metal catalyst carrier medium and the performance of the degradation process is indirectly affected by the carbon material. Polymer-based porous carbon can be used as an adsorbent in adsorption and a metal catalyst carrier medium in degradation process. Porous carbon made by the carbonization process of synthetic polymers can produce a more uniform structure (Rajagopal et al. 2020). The pore size can be adjusted by changing the polymer precursor and can have a large specific area (Prasetyo et al. 2013).

The paper presents a study of synthesis iron oxide on porous carbon material as an alternative method for removal metronidazole concentration in water by adsorption process and then followed by a degradation process using AOPs. Porous carbon material was produced by carbonization of synthetic polymer due to the pore size can be turned by alter polymeric precursors. To determine the performance of the catalytic system of porous carbon as a carrier medium, AOPs using hydrogen peroxide (heterogeneous Fenton) and Ozonation catalytic ozone will be used, and the results will be compared. Porous carbon will be tested for stability as a catalyst with repeated use of four processes in a row.

2. EXPERIMENT SECTION.

2.1 Materials

The carbon support used in this study was polymer derived carbon synthesized by pyrolysis of resorcinol and formaldehyde. $Fe(NO_3).9H_2O$ (99% purity Merck, Germany) was employed as iron oxide precursor. In the degradation processes, metronidazole (99% Sigma Aldrich, Singapore) was used as a target pollutant. H_2O_2 (50% purity) from Merck and Ozone from ozonation generator, were used as a hydroxyl radical producer.

2.2 Carbon catalyst preparation

Porous carbon was synthesized by pyrolysis of phenolic resin. To produce polymeric mixture resorcinol, formaldehyde, with and without $Fe(NO_3).9H_2O$. The molar ratio of resorcinol and formaldehyde was fixed to 2.8:1. The mass fraction of catalyst precursor ($Fe(NO_3)_3.9H2O$) was 1% of the total solution. Polycondensation reaction of polymer precursor mixture was described elsewhere (Prasetyo et al. 2013). Polymer material was placed in the furnace and then the furnace was heated to 800 °C with ramp rate of 3 °C, and under nitrogen atmosphere. The furnace was cooled down to ambient temperature overnight. Porous carbon without and with iron oxide/carbon were labeled as blank carbon and Fe/C, respectively.

2.3 Adsorption test

The metronidazole adsorption was performed through a preparation of metronidazole solution at various concentrations. The initial concentration range from 0 to 800 ppm was employed to determine adsorbate in liquid and solid phase, until the adsorption capacity was reached. A 50 mg carbon was poured into 50 ml metronidazole solution placed in Erlenmeyer. The mixture was shaken for 24 h in a water bath shaker (Memmert, Schwabach, Germany) at 30 °C until equilibrium. The sample was mixed with 1 M HCl, $NaNO_2$, sulfamic acid dan b-naphthol. A 1 M NaOH was then added till the solution was colored. The metronidazole adsorption test in liquid was performed using a Vis Spectrophotometer (C-7000 Series Spectrophotometer, Peak Instrument Inc) at λ_{max} from the previously determined calibration curve (wavelength of 510 nm). The detail of adsorption method and analytical method are provided in literature (Panandita 2022; Saffaj et al. 2006). The uptake capacity (C_μ) was calculated by mass balance formulation of Eq. (1).

$$C_\mu = \frac{(C_0 - C_e) \times V}{m} \quad (1)$$

Where C_0 is the initial concentration of metronidazole in the liquid phase ($mg.L^{-1}$), C_e is equilibrium concentration of metronidazole in the liquid phase ($mg.L^{-1}$) after adsorption, m is the mass of adsorbent (g) and V is the volume of the solution (L). Equilibrium data were modeled using Langmuir and Freundlich models, as show in Eq. (2) and Eq. (3).

$$C_\mu = \frac{C_{\mu max} \times K_L \times C_e}{1 + K_L \times C_e} \quad (2)$$

$$C = K_F \times C_e^{1/n} \quad (3)$$

Where $C_{\mu max}$ is the maximum adsorption capacity ($mg.g^{-1}$ carbon), K_L and K_F are the Langmuir and Freundlich equilibrium constant, respectively.

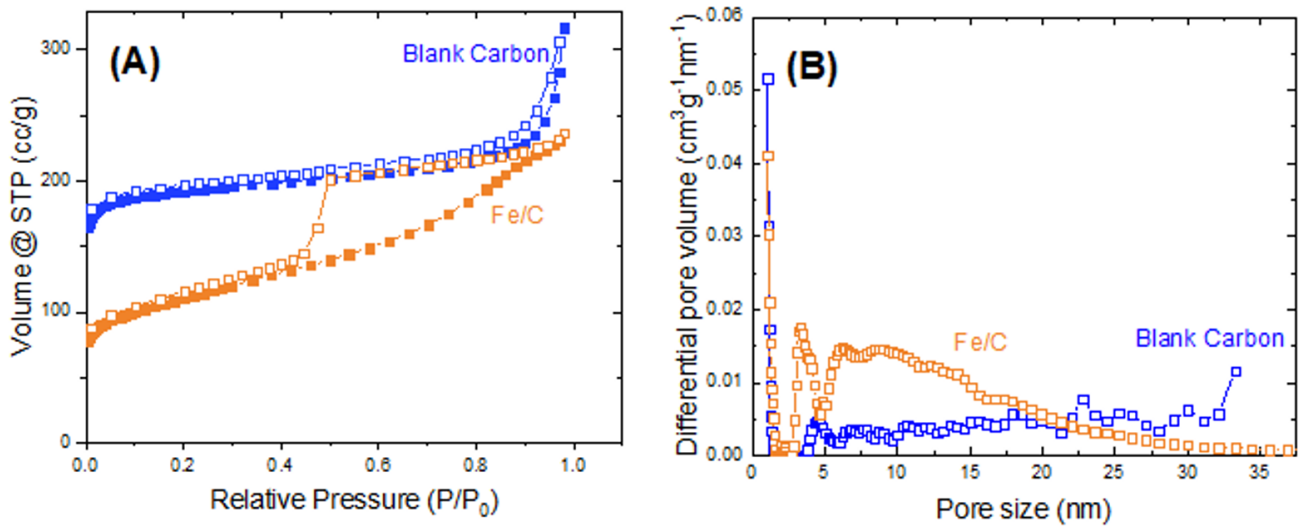

FIGURE 2. (a) N_2-sorption isotherm (closed symbol: adsorption, open symbol: desorption) and (b) pore size distribution of blank carbon and Fe/C.

2.4 Degradation test

Carbon material used in adsorption was placed in a three-neck flask containing 100 ml aquadest. The solution was stirred at a constant speed at a room temperature (about 30 °C). Then, oxidation of AOPs (H_2O_2 and ozone) were added into the three-neck flask while stirring for 4 h (used H_2O_2) and 2 h (used ozone and combination process). Residual concentration of H_2O_2 was analyzed spectrophotometrically by the titanium oxysulfate method (1.5-2.0 Ti based as TiO_2). The concentration of metronidazole detected in liquid phase was determined by Vis Spectrophotometer (C-7000 Series Spectrophotometer, Peak Instrument Inc.) at a wavelength 510 nm. The degradation test was conducted in 5 cycles using the same Fe/C material to evaluate the efficacy of the catalyst for consecutive usage. Fe/C was dried in oven at 60 °C prior to the next run. The detail procedures are provided in literature (Panandita 2022).

2.5 Characterization methods

The porosity of the porous carbon (Fe/C and blank carbon) was characterized by nitrogen physisorption at a temperature of 77K using a Quantachrome instrument (NOVA 2000, USA). The analytical method used was multipoint Brunauer-Emmett-Teller (BET) to determine the specific surface area. The pore size distributions (PSDs) were evaluated using the Density Functional Theory (DFT) model. The morphology of the carbon surface material was observed by Scanning Electron Microscopic (SEM, JEOL JSM-6510 LA). Energy Dispersive X-ray (EDX) coupled with SEM was used to investigate chemical elemental materials.

3. RESULT AND DISCUSSION

3.1 Pore structures of materials

The type of material used will affect the structure of the pore characteristics with different pore properties. This difference will later affect the adsorption and degradation performance and the effect of the iron oxide catalyst on the carbon characteristics. The material properties of the porous carbon material were characterized using low-temperature nitrogen physisorption analysis. Figure 2.a displays the result of the sorption isotherm. According to the International Union of Pure and Applied Chemistry (IUPAC) classification (Thommes et al. 2015), the shape of the isotherm for Fe/C is classified as a combination of type I and IV isotherm. This means an unrestricted monolayer-multilayer adsorption with a hysteresis loop. While blank carbon is classified

TABLE 1. Analysis result of pore properties.

Material	SSA[a] (m^2g^{-1})	V_s[b] (cm^3g^{-1})	$\%V_{mic}$[c] (%)	d_v[d] (nm)
Blank Carbon	755	0.49	55.05	2.61
Fe/C	394	0.37	22.02	3.72

[a]Specific surface area, determined by multipoint BET
[b]Total pore volume at 0.98 P/P_0
[c]Micropore volume fraction, determined by the *t-plot* method
[d]Mean pore diameter, calculated with $d_v = 4V_t/area$

TABLE 2. Constant value of various fitting models of metronidazole adsorption.

Material	Langmuir model			Freundlich model		
	K_L (Lmg^{-1})	$C_{\mu max}$ (mg g ^{1})	R^2	k_f	n	R^2
Blank carbon	0.00351 ±0.0064	39.97 ±4.25	0.96	1.08 ±0.52	1.98 ±0.32	0.96
Fe/C	0.0354 ±0.0041	46.07 ±0.004	0.99	15.40 ±1.43	5.87±0.56	0.99

 DOI 10.22146/jrekpros.75633

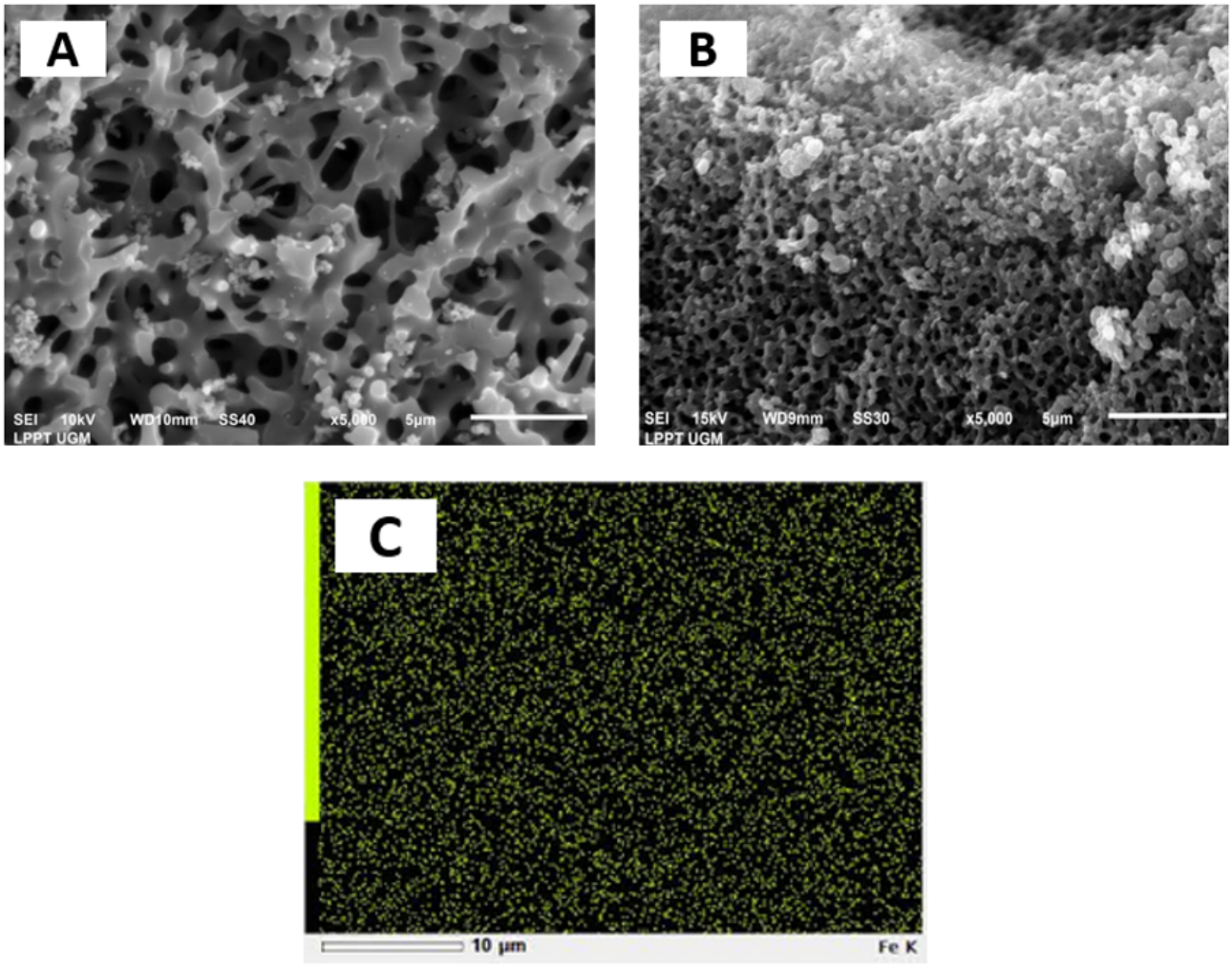

FIGURE 3. The SEM images of blank carbon (a), Fe/C material (b) and elemental mapping (EDX) of Fe in carbon (c).

as a microporous material (Type I). This can be seen from the adsorption line which approached a saturation value at small P/Po. N_2-uptake capacities of both carbons indicates that highly porous material is present. The pore size distributions (PSDs) calculated with the DFT model Figure 2.b The pore size was distributed to the porous carbon with iron oxide catalyst having a higher mesopore fraction (2-5 nm). On the other hand, the blank porous carbon, which had a reasonably high micropore fraction (2 nm).

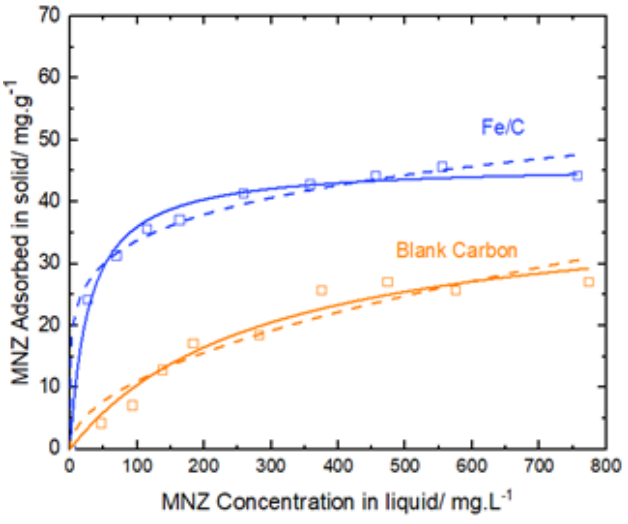

FIGURE 4. Adsorption isotherm of metronidazole in blank carbon and Fe/C (line: Langmuir fitted curve; dash line: Freundlich fitted curve).

The structural properties of the two carbon materials such as specific surface area (SSA), pore volume, average pore size, and microporosity are summarized in Table 1. This table compares the results of carbon added with and without iron oxide catalyst. The textural properties showed that surface area (394-754 m^2g^{-1}) and a highly developed porosity are obtained. This material could be compared with porous carbon synthesized from other polymeric materials, which are usually produced in the range of 600-2000 m^2 g^{-1}. For Fe/C, the reduction of the specific surface area is likely due to the iron oxide in the material, which is non-porous and can induce mesoporous-graphitic structure (Prasetyo et al. 2019; Amelia et al. 2020). Fe/C and blank carbon material have mesoporous structure with a mean pore 3.72 nm and 2.61 nm. The difference can occur due to the presence of iron oxide and high temperature process that triggers a mesoporous structure. Comparing the total pore volume of both carbon materials, the iron oxide carbon material featured a higher pore volume (0.491 cm^3g^{-1}) than blank carbon (0.367) cm^3g^{-1}. Overall, the results from the porosity analysis of blank carbon have a larger specific surface area, but the Fe/C material have a larger mesopore size.

3.2 Surface morphologies and elemental analysis

The morphology of carbon material was investigated using scanning electron microscopy. From Fig 3.a and Fig 3.b, SEM images showed that surface of the Fe/C material has more voids than the blank carbon. It is important to mention that pore sizes which are important for molecular adsorption are in the range of nanometer scale, hence it is unseen in the SEM images. The results indicate that the addition of iron oxide can affect the morphology of carbon surface. This relates to the use of polymer precursor types and their composition (Asgharzadeh et al. 2020). To determine the distribution of iron on the carbon surface, Fe elemental mapping by EDX was carried out as can be seen in Figure 3.c. The color in the image from elemental mapping (EDX) indicates the presence of Fe on the carbon surface. It shows that the iron oxide has been distributed well. In other words, the result clearly showed successful preparation steps to produce iron oxide porous carbon material.

3.3 Metronidazole adsorption

The performance of material was tested in the metronidazole adsorption in the range of 0-800 ppm metronidazole solution (Figure 4). Metronidazole can be adsorbed by both carbon material of Fe/C and blank carbon. The adsorption performance of iron oxide carbon is slightly better than the blank carbon in the term of uptake capacity. For blank carbon, the uptake capacity is ca. 25 mg g^{-1} at 800 ppm. The impregnation of iron oxide loading remarkably increases the metronidazole adsorption, which results in ca 40 mgg^{-1}.

Isotherm models have been reported to represent the adsorption equilibrium data. In this study, the Langmuir isotherm model and Freundlich isotherm model were fitted to the experimental metronidazole adsorption data for both materials. These adsorption isotherms can be represented mathematically by Eq. (2) and (3). The parameters of models are shown in Table 2. The Langmuir models are more appropriate for metronidazole adsorption models than Freundlich models (R^2 closer to 1). The parameter $C_{\mu max}$ is the maximum adsorption capacity. For iron oxide carbon material, the value of the maximum adsorption capacity for Langmuir model 46.07 mg/g at 800 ppm, which is higher than blank carbon material (39.97 mg g^{-1}). The value of Langmuir constant of K_L for F/C is higher than blank carbon. It is likely that uptake capacity of metronidazole seems to be more related to change in pore textural properties (Table 1). Blank carbon has a low mean pore size which hindered adsorption despite having a high specific surface area. This effect to adsorption metronidazole is in agreement with literatures (Carrales-Alvarado et al. 2014).

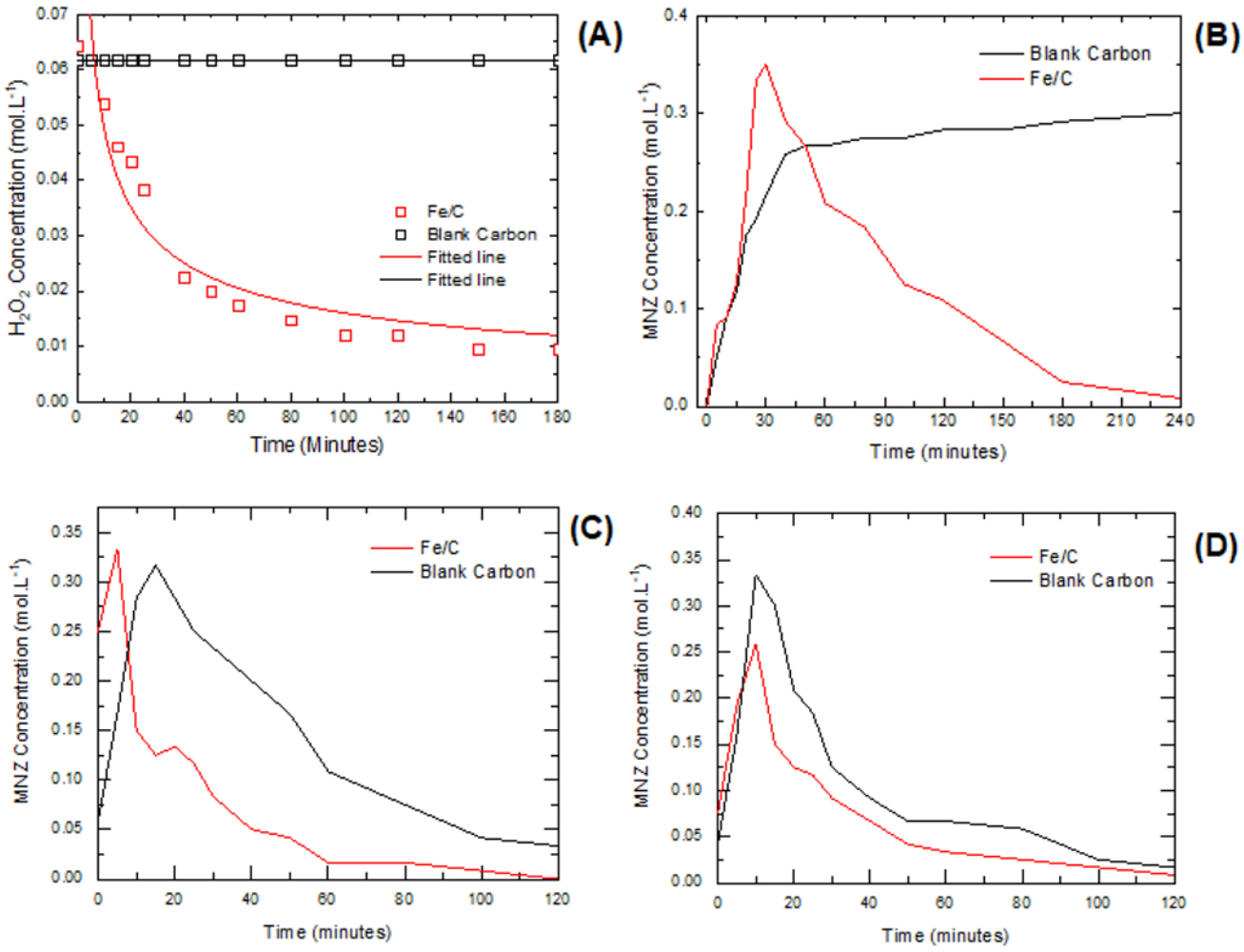

FIGURE 5. Concentration profile of H_2O_2 (a), Concentration profile of metronidazole in liquid phase during H_2O_2 method (b) Concentration profile of metronidazole in liquid phase during ozonation (c) Concentration profile of metronidazole in liquid phase during H_2O_2/O_3 method (d) Condition: 100mg of catalyst in 100 mL solution and 30 °C reaction temperature.

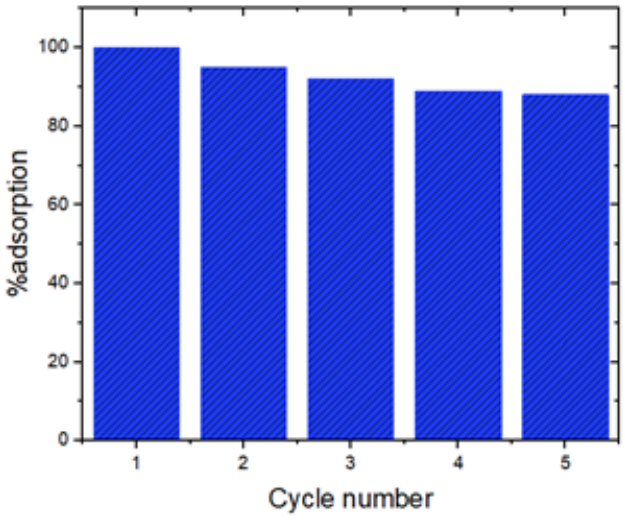

FIGURE 6. Durability test showing high reusability of Fe/C for metronidazole removal.

3.4 Catalytic degradation performance

The performance of material was then studied in degradation test to evaluate the role of carbon material as a catalyst. The adsorbent that had previously been used in the adsorption process were separated and then degraded by heterogeneous Fenton, Catalytic ozonation and ozone/H_2O_2 methods. As observed Figure 5.a, the experiment with blank carbon and Fe/C in H_2O_2 solution was performed to evaluate the possible role of Fe/C material as catalyst. The experimental data was fitted by considering the first order of reaction for H_2O_2 depletion. It can be seen that no significant decrease of H_2O_2 was observed after 3 h reaction time using blank carbon. It concluded that blank carbon cannot facilitate the formation of hydroxyl radicals. On the other hand, Fe/C material can facilitate the formation of hydroxyl radical in the 30 min regarding the decrease of H_2O_2 concentration profile. In Figure 5.b, the metronidazole concentration was observed after 4 h reaction time using H_2O_2. It can be determined that H_2O_2 cannot oxidize the metronidazole without catalyst Fe under the operating conditions in this work. The degradation process with blank carbon only desorbs metronidazole back into liquid phase. However, there is a 79% reduction of metronidazole when using oxidizing H_2O_2 and catalyst Fe/C. The transfer of metronidazole from adsorbent to liquid can occur due to the influence of stirring condition during degradation process. This was because metronidazole molecules were in solid phase, so the metronidazole concentration cannot be measured directly.

The degradation result of metronidazole with Fe/C and blank carbon material through O_3 and O_3/H_2O_2 is shown in Figure 5.c and Figure 5.d, the results presented show that degradation allows of each material. In the blank carbon material, there was decrease in the concentration of metronidazole during a 2-h process. This is likely due to the ozone is an oxidizing agent with high oxidation potential (2.07 V) and could break the chemical bonds of organic molecules directly (Issaka et al. 2022). However, the oxidizing is lower than hydroxyl radical. The presence of iron oxide catalyst (Fe/C) in the degradation processes can accelerate the degradation process. This effect to degradation using O_3 is also observed from literature (Nasseh et al. 2020).

The results showed that degradation using O_3 and O_3/H_2O_2 with Fe/C material showed a reduction of metronidazole reaching almost 90%. The reduction of metronidazole is better when using Fe/C and combination of O_3/H_2O_2. Metronidazole was fully degraded at 2 h. This was due to the very strong oxidative properties of the hydroxyl radicals produced from hydrogen peroxide and catalyst (He et al. 2016) and the reaction of O_3/Fe^{2+}, O_3/H_2O_2 and H_2O_2/Fe^{2+} yielded a large amount hydroxyl radicals. This indicates Fe/C could be used as a catalyst in the degradation of metronidazole using AOPs.

3.5 Recyclability test of Fe/C catalyst

To evaluate the reusability of material, Fe/C was submitted to consecutive adsorption and degradation runs (H_2O_2/O_3). The degradation was achieved after 2 h reaction time along for 4 runs. The result is shown in Figure 6. According to adsorption process, its slight decrease in repetitions (about 12%). The decrease in adsorption performance of Fe/C in consecutive tests can be caused by remaining metronidazole in the solid carbon. Therefore, material is not able to adsorb metronidazole as much as the previous process. This effect of using Fe/C material synthesized by phenolic resin is also observed from literature (Amelia et al. 2020). In general, the Fe/C material synthesized from resorcinol-formaldehyde has a good physical resistance as shown by only ca. 10% decrease in adsorption performance.

4. CONCLUSIONS

Fe/C catalyst was produced by impregnation of iron oxide precursor in polymerization of resorcinol formaldehyde followed by pyrolysis. Fe/C exhibited dominantly mesoporous with the specific surface area of 394 mg^2g^{-1}, while blank carbon dominantly displayed microporous with the specific surface area higher than Fe/C (755 mg^2g^{-1}). Iron oxide could be successfully loaded in the porous carbon material as proven by result of SEM-EDX analysis. Uptake measurement exhibited that metronidazole is more favorably adsorbed in Fe/C. The Fe/C catalyst showed high stability and maintained its activity almost unchanged consecutive runs.

ACKNOWLEDGMENTS

The authors thank Kurita Overseas Research Grant 2021 (21Pid077-17 T) for the provided funding.

REFERENCES

Amelia S, Sediawan WB, Prasetyo I, Munoz M, Ariyanto T. 2020. Role of the pore structure of Fe/C catalysts on heterogeneous Fenton oxidation. Journal of Environmental Chemical Engineering. 8(1):102921. doi:10.1016/j.jece.2019.102921.

Ariyanto T, Kurniasari M, Laksmana WT, Rochmadi, Prasetyo I. 2019. Pore size control of polymer-derived carbon adsorbent and its application for dye removal. International Journal of Environmental Science and Technology. 16(8):4631–4636. doi:10.1007/s13762-018-2166-0.

Asgharzadeh F, Gholami M, Jafari AJ, Kermani M, Asgharnia H, Kalantary RR. 2020. Heterogeneous photocatalytic

degradation of metronidazole from aqueous solutions using Fe_3O_4/TiO_2 supported on biochar. Desalination and Water Treatment. 175:304–315. doi:10.5004/dwt.2020.24789.

Balarak D, Khatibi AD, Chandrika K. 2020. Antibiotics removal from aqueous solution and pharmaceutical wastewater by adsorption process : A review. 10(2):106–111. doi:10.5530/ijpi.2020.2.19.

Carrales-Alvarado DH, Ocampo-Pérez R, Leyva-Ramos R, Rivera-Utrilla J. 2014. Removal of the antibiotic metronidazole by adsorption on various carbon materials from aqueous phase. Journal of Colloid and Interface Science. 436:276–285. doi:10.1016/j.jcis.2014.08.023.

Costanzo SD, Murby J, Bates J. 2005. Ecosystem response to antibiotics entering the aquatic environment. 51:218–223. doi:10.1016/j.marpolbul.2004.10.038.

Cuerda-Correa EM, Alexandre-Franco MF, Fernández-González C. 2020. Advanced oxidation processes for the removal of antibiotics from water. An overview. Water (Switzerland). 12(1). doi:10.3390/w12010102.

Escher BI, Baumgartner R, Koller M, Treyer K, Lienert J, Mcardell CS. 2010. Environmental toxicology and risk assessment of pharmaceuticals from hospital wastewater. Water Research. 45(1):75–92. doi:10.1016/j.watres.2010.08.019.

Gadipelly C, Pérez-González A, Yadav GD, Ortiz I, Ibáñez R, Rathod VK, Marathe KV. 2014. Pharmaceutical industry wastewater: Review of the technologies for water treatment and reuse. Industrial and Engineering Chemistry Research. 53(29):11571–11592. doi:10.1021/ie501210j.

Goolsby TA, Jakeman B, Gaynes RP. 2018. Clinical relevance of metronidazole and peripheral neuropathy: a systematic review of the literature. International Journal of Antimicrobial Agents. 51(3):319–325. doi:10.1016/j.ijantimicag.2017.08.033.

He J, Yang X, Men B, Wang D. 2016. Interfacial mechanisms of heterogeneous Fenton reactions catalyzed by iron-based materials: A review. Journal of Environmental Sciences (China). 39:97–109. doi:10.1016/j.jes.2015.12.003.

Ighalo JO, Igwegbe CA, Adeniyi AG, Adeyanju CA, Ogunniyi S, Ighalo JO, Igwegbe CA, Adeniyi AG. 2020. Mitigation of Metronidazole (Flagyl) pollution in aqueous media by adsorption : a review. doi:10.1080/21622515.2020.1849409.

Issaka E, AMU-Darko JNO, Yakubu S, Fapohunda FO, Ali N, Bilal M. 2022. Advanced catalytic ozonation for degradation of pharmaceutical pollutants—A review. Chemosphere. 289(December 2021). doi:10.1016/j.chemosphere.2021.133208.

Johnson MB, Mehrvar M. 2008. Kinetics , catalysis , and reaction engineering aqueous metronidazole degradation by UV / H2O2 process in single-and multi-lamp tubular photoreactors : jinetics and reactor design:6525–6537. doi:10.1021/ie071637v.

Malakootian M, Kannan K, Gharaghani MA, Dehdarirad A, Nasiri A, Shahamat YD, Mahdizadeh H. 2019. Removal of metronidazole from wastewater by Fe/charcoal micro electrolysis fluidized bed reactor. Journal of Environmental Chemical Engineering. 7(6):103457. doi:10.1016/j.jece.2019.103457.

Mirzaei A, Chen Z, Haghighat F, Yerushalmi L. 2017. Removal of pharmaceuticals from water by homo/heterogonous Fenton-type processes – A review. Chemosphere. 174:665–688. doi:10.1016/j.chemosphere.2017.02.019.

Mohd Zawawi N, Hamzah F, Veny H, Mohd Rodhi MN, Sarif M. 2021. Chemical and electrochemical properties of bamboo activated carbon activate using potassium hydroxide assisted by microwave-ultrasonic irradiation. ASEAN Journal of Chemical Engineering. 21(2):211–224. doi:10.22146/ajche.64617.

Munoz M, Mora FJ, de Pedro ZM, Alvarez-Torrellas S, Casas JA, Rodriguez JJ. 2017. Application of CWPO to the treatment of pharmaceutical emerging pollutants in different water matrices with a ferromagnetic catalyst. Journal of Hazardous Materials. 331:45–54. doi:10.1016/j.jhazmat.2017.02.017.

Nasseh N, Arghavan FS, Rodriguez-Couto S, Hossein Panahi A, Esmati M, A-Musawi TJ. 2020. Preparation of activated carbon@ZnO composite and its application as a novel catalyst in catalytic ozonation process for metronidazole degradation. Advanced Powder Technology. 31(2):875–885. doi:10.1016/j.apt.2019.12.006.

Panandita B. 2022. Adsorpsi metronidazol dengan adsorben fexoy/c dan degradasinya dengan Fenton heterogen serta ozonasi katalitik. [Master's thesis]: Universitas Gadjah Mada.

Patel M, Kumar R, Kishor K, Mlsna T, Pittman CU, Mohan D. 2019. Pharmaceuticals of emerging concern in aquatic systems: Chemistry, occurrence, effects, and removal methods. Chemical Reviews. 119(6):3510–3673. doi:10.1021/acs.chemrev.8b00299.

Prasetyo I, Fajar Mukti NI, Ariyanto T. 2019. Ethylene adsorption using cobalt oxide-loaded polymer-derived nanoporous carbon and its application to extend shelf life of fruit. Molecules. 24(8). doi:10.3390/molecules24081507.

Prasetyo I, Rochmadi, Ariyanto T, Yunanto R. 2013. Simple method to produce nanoporous carbon for various applications by pyrolysis of specially synthesized phenolic resin. Indonesian Journal of Chemistry. 13(2):95–100. doi:10.22146/ijc.21290.

Rajagopal V, Kathiresan M, Manivel P, Suryanarayanan V, Velayutham D, Ho KC. 2020. Porous organic polymer derived metal-free carbon composite as an electrocatalyst for CO_2 reduction and water splitting. Journal of the Taiwan Institute of Chemical Engineers. 106:183–190. doi:10.1016/j.jtice.2019.10.016.

Saffaj T, Charrouf M, Abourriche A, Aboud Y, Bennamara A, Berrada M. 2006. Spectrophotometric determination of Metronidazole and Secnidazole in pharmaceutical preparations based on the formation of dyes. Dyes and Pigments. 70(3):259–262. doi:10.1016/j.dyepig.2005.01.009.

Seidmohammadi A, Vaziri Y, Dargahi A, Nasab HZ. 2021. Improved degradation of metronidazole in a heterogeneous photo-Fenton oxidation system with PAC/Fe3O4 magnetic catalyst: biodegradability, catalyst specifications, process optimization, and degradation pathway. Biomass Conversion and Biorefinery. (0123456789). doi:10.1007/s13399-021-01668-7.

Thommes M, Kaneko K, Neimark AV, Olivier JP, Rodriguez-Reinoso F, Rouquerol J, Sing KSW. 2015. Physisorption of gases, with special reference to the evaluation of sur-

face area and pore size distribution (IUPAC Technical Report). Pure and Applied Chemistry. 87(9-10):1051–1069. doi:10.1515/pac-2014-1117.